Journal of Electronic Materials (2023) 52:3774–3785
https://doi.org/10.1007/s11664-023-10338-5

ORIGINAL RESEARCH ARTICLE

Molecular Screening of Different π-Linker-Based Organic Dyes for Optoelectronic Applications: Quantum Chemical Study

Arunkumar Ammasi[1] · Ragavan Iruthayaraj[1] · Anbarasan Ponnusamy Munusamy[1] · Mohd Shkir[2,3] · Balasubramani Vellingiri[4] · Vasudeva Reddy Minnam Reddy[5] · Woo Kyoung Kim[5]

Received: 31 October 2022 / Accepted: 28 February 2023 / Published online: 25 March 2023

Abstract

In this work, metal-free organic dyes (SZ-1–SZ-5) based on phenothiazine (PTZ) as donor (D) unit and different π-conjugated (π) as spacers and acceptors (A) representing cyanoacetic acid (D-π-A) have been investigated to examine their optoelectronic properties by density functional theory (DFT) and time-dependent DFT (TD-DFT) calculations. A favourable electron transfer into the semiconducting material (TiO_2) is effectively obtained by the optimized ground state HOMO-LUMO energy values of the SZ-3 molecule. The photovoltaic (PV) parameters of the oxidation and reduction potential energies (E^{dye} and E^{dye^*}), a driving force of electron injection (ΔG_{inject}), dye regeneration (ΔG_{reg}), light-harvesting efficiency (*LHE*), dipole moment (μ_{normal}), short-circuit current density (J_{SC}) and open-circuit photovoltage (eV_{OC}) were obtained and are discussed in detail. On the other hand, the TD-DFT approach was used to calculate and describe the optical properties of all SZ-1–SZ-5 molecules in terms of absorption energy associated with maximum wavelengths (λ_{max}), emission spectra (λ_{emi}), oscillator strengths (*f*) and excitation energies (*E*). Finally, the theoretical findings represent the various π-spacers in the optoelectronic capabilities of the D-π-A-based dye derivative materials, and they offer useful guidelines for future structures designed for solar cell applications.

Keywords DFT and TD-DFT · DSSCs · free energy charge of electron injection · π-linkers · PV

Introduction

One of the greatest innovative technologies and scientific difficulties in the contemporary era has been the creation of highly efficient solar photovoltaic (PV) systems due to the growing environmental pollution and the depletion of fossil fuels (coal, oil, and gas). Since Grätzel and O'Regan published their first successful demonstration of dye-sensitized solar cells (DSSCs) as a low-cost alternative to the highly efficient PV cells in 1991, DSSCs have gained considerable attention as a potential low-cost PV cell replacement.[1–4] Ru-based complexes are reported to have the best solar power conversion efficiency (PCE), which is over 12% under a calibrated AM 1.5 radiation, despite their high cost and environmental concerns.[5] However, the Ru-compounds are very costly, with a low molar extinction coefficient and difficult purification steps. However, there is a critical need for metal-free organic dyes targeted at DSSCs without noble metals. Researchers are now looking more closely at the connection between dye chemical systems and their PV performance as

✉ Arunkumar Ammasi
arunkumara.phys@gmail.com

✉ Anbarasan Ponnusamy Munusamy
profpmanbarasan@gmail.com

Vasudeva Reddy Minnam Reddy
drmvasudr9@gmail.com

1 Department of Physics, Periyar University, Salem 636 011, India

2 Research Center for Advanced Materials Science (RCAMS), King Khalid University, Abha 61413, Saudi Arabia

3 University Center for Research & Development (UCRD), Chandigarh University, NH95, Chandigarh-Ludhiana Highway, Gharuan, Mohali, Punjab 140413, India

4 Department of Physics, Saveetha School of Engineering, Saveetha Institute of Medical and Technical Sciences, Chennai, Tamilnadu 602 105, India

5 School of Chemical Engineering, Yeungnam University, Gyeongsan 38541, Republic of Korea

a result of the recent success of PCE for DSSCs based on organic sensitizers.[6,7]

The majority of organic sensitizers nowadays have a donor-spacer-acceptor (D-π-A) molecular architecture, where the electron-donor (D) and electron-acceptor (A) are both coupled to the π-spacer molecular system. In addition to the wide range of molecular systems available, it has great efficiency, cheap cost, good flexibility, and abundance of raw materials. But there are still issues to be overcome with the decreased energy efficiency of metal-free organic dyes, thermal energy-harvesting devices and electrochemical stability. To achieve high performance of the PV devices, it is important to discover D-π-A types of dye sensitizers. For DSSCs, organic dye molecules containing a variety of heterocyclic building blocks have been described, including triphenylamine, fluorine, carbazole, tetrahydroquinoline, anthracene, N,N-dialkylaniline, merocyanine and coumarin.[8–16]

Particularly, the most widely used phenothiazine (PTZ) and its derivatives are utilized in industrial dyes, optical brightening agents (OBAs), scintillators, fluorescent brightening agents, extremely bioactive substances, and many other things. Because it plays a significant role in electrochemistry and numerous photophysical and photochemical oxidation devices, the synthetic derivative of PTZ has been gaining interest for more than half a century.[17,18] Because of their low processing cost, ab initio calculations and molecular simulations have emerged as crucial tools for solving molecular problems and interpreting experimental data.[19–25] The enhancements in CPU resources now make it possible to simulate the electrical characteristics of large-scale dye material behaviours.[26–29] One of the most popular methods for these computations is time-dependent self-consistent-field (TD-SCF), which offers significantly better agreement with observed data for a justifiable computational conclusion, especially when hybrid exchange–correlation (XC) functionals are employed.[30–32] It is acknowledged that the thiazine class of heterocyclic chemicals, such as PTZ derivatives, may prove difficult to study using quantum theory. The dye sensitizer (E)-3-(10-butyl-10H-phenothiazin-3-yl)-2-cyanoacrylic acid (T2-1) published by Sun and co-authors in 2007 comprises PTZ and 2-cyanoacrylic acid, which serve as electron-D and electron-A (D-A) groups. [33] This kind of sensitizer causes a shift in surface charge that significantly decrease dye recombination in its excited state and hence improves the solar PV efficiency in their DSSCs. A well-known family of electron-rich heterocyclic thiazine compounds called PTZ dye has become established in organic solar cells due to its special features. In DSSCs, for instance, PTZ-based D-A-π-A dyes of PZ-1-4 have been developed and are known for their high photocurrent performance.[34]

In light of the study approach previously stated, we attempted to combine all the intriguing characteristics of PTZ derivatives in comparison to the T2-1 molecule. Appropriately varied π-conjugated spacers (SZ-1–SZ-5) molecular structures were depicted in Scheme 1. According to the plan, the π-spacer groups provide a chance to carry out computational research using D-π-A architecture for the development of more effective PTZ dye. Additionally, the effect of SZ-1–SZ-5 dyes on semiconductor and PV characteristics was examined. We seek to establish the essential connections between the structure–property of various π-spacer dyes and the development of optoelectronics with high energy conversion efficiencies using theoretical simulations.[35–37]

Computational Aspects

The Gaussian 09w[38] software package carried out all computations using a hybrid Becke-3-Lee–Yang–Parr (B3LYP) functional with a 6-31G(d,p) basis set. Utilizing the hybrid B3LYP theory and quantum chemical computations, the ground state geometries (S0) of all the specified dyes were calculated.[39,40] To calculate the electronic absorption and emission spectra with the excited state of all SZ-1–SZ-5 dyes, time-dependent DFT (TD-DFT) computations were used. Those spectra were pictured by GaussSum version 3.0 software. The energy gap (E_g) and electron densities of the highest occupied molecular orbital (HOMO) and lowest unoccupied MO (LUMO) levels of the SZ-1–SZ-5 molecules were calculated using the same method. The above approaches are also used to estimate the polarizability of the first static (hyper) polarizability of the non-linear optical (NLO) investigation for its optoelectronic properties. Moreover, the oscillator strength (*f*) acquired by using the TD-DFT approach is used to compute light harvesting efficiency (*LHE*).

Results and Discussion

Screening of π-Conjugated Bridge

A major problem with the D-π-A framework for the PV performance of DSSCs, as we described in the previous section, led us to change the π-spacer in particular. We calculated SZ-1 to SZ-5 dyes based on T2-1 dye in order to demonstrate good PV performances of the various conjugated systems of PTZ-based metal-free dyes. The subsequent inclusion of various functional groups, including thieno[3,4-d]pyrimidine, thieno[3,4-b][1,4]dioxine, 2,5-thiophenedicarboxaldehyde, benzo[c][1,2,5]thiadiazole and [1,2,5]thiadiazolo[3,4-g]quinoxaline. Figure 1 illustrates the influence of the superior π-spacer portions on the structural geometries for all the SZ-1 to SZ-5 dyes. Table I displays the calculated geometrical parameters of some important torsion angles or dihedral angles of the molecules. The computed results shown in

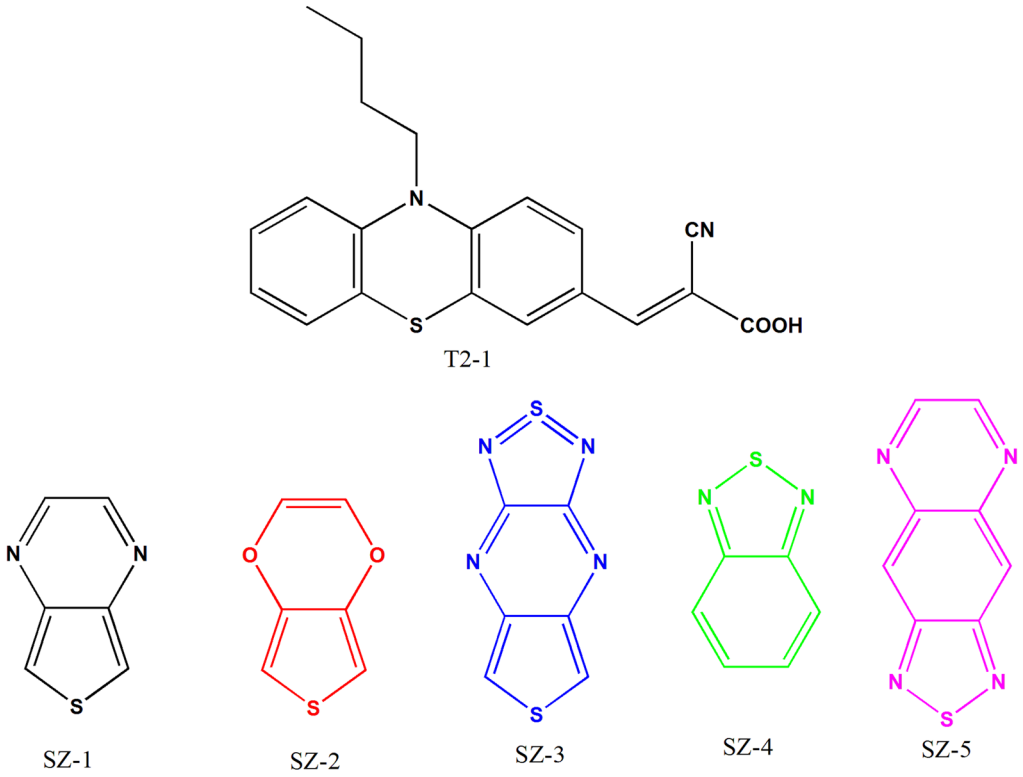

Scheme 1 Structures of designed metal-free organic dyes.

Table I demonstrate that the SZ-1–SZ-5 dyes have superior delocalized electron distributions compared to T2-1 dye and are hence more amenable to better intramolecular charge transfer (ICT) capabilities.

Electronic Structure of the Dyes

To examine the optical and electrical characteristics of SZ-1–SZ-5 molecules, the TD-DFT approach was used. Using the conductor-like polarized continuum model (CPCM), the initial self-consistent field (SCF) predicted by hybrid B3LYP level theory at 6-31G(d,p) basis sets was used to determine the solvation of free energies. The ultraviolet–visible (UV–Vis) spectral analysis of the developed dyes must be associated with considerable absorption capacity and must fit as closely as feasible with the solar radiation spectrum. Figure 2 shows the simulated absorption spectra of the SZ-1–SZ-5 dyes. Table II shows the results of TD-DFT calculations on the excitation energies (E), f and electronic transitions to provide insight into the electronic and photophysical characteristics of SZ-1–SZ-5 molecules and T2-1. Using T2-1 as a reference dye molecule, the normalized absorption wavelengths from 300 nm to 800 nm are also determined in order to take a relative position of the strong absorption quality and ability of all provided dyes in the visible range. These dye molecules absorb light at two separate wavelengths (λ_{max}) in the UV and visible light spectrum. The π-π* electronic transitions are responsible for the shorter λ_{max} range between 300 nm and 400 nm, while it is acknowledged that the organic D-A electron transfer state occurs in the longer λ_{max} range of 600–900 nm. According to calculations, the highest λ_{max} for SZ-3 occurs at 810 nm, with an electronic excitation energy of 1.531 eV. When compared to the T2-1 dye, the HOMO → LUMO with f of 0.197 are responsible for a 100% substantial contribution to this electronic transition. Additionally, the second-best λ_{max} peak at 680 nm (SZ-1) with an f of 0.181 is assumed to be mostly caused by the HOMO → LUMO transition. To put it another way, it was discovered that the length of π-conjugation increased and the optical absorption range shifted to higher λ_{max} as a result of metal-free organic substitution. These PTZ derivatives are good options for increasing solar light harvesting in the infrared (IR) region of the solar spectrum for use in PV solar cells.

The emission spectra (λ_{emi}) of dye sensitizers based on PTZ were determined using TD-DFT computations. All dyes were exposed to emission spectra using the optimized geometry of the excited state and the corresponding values of electronic transition, λ_{emi} and other parameters are tabulated in Table III. The estimated emission spectra of PTZ-based SZ-1–SZ-5 dye sensitizers in THF solvent are displayed in Fig. 3. These dyes will have good fluorescence

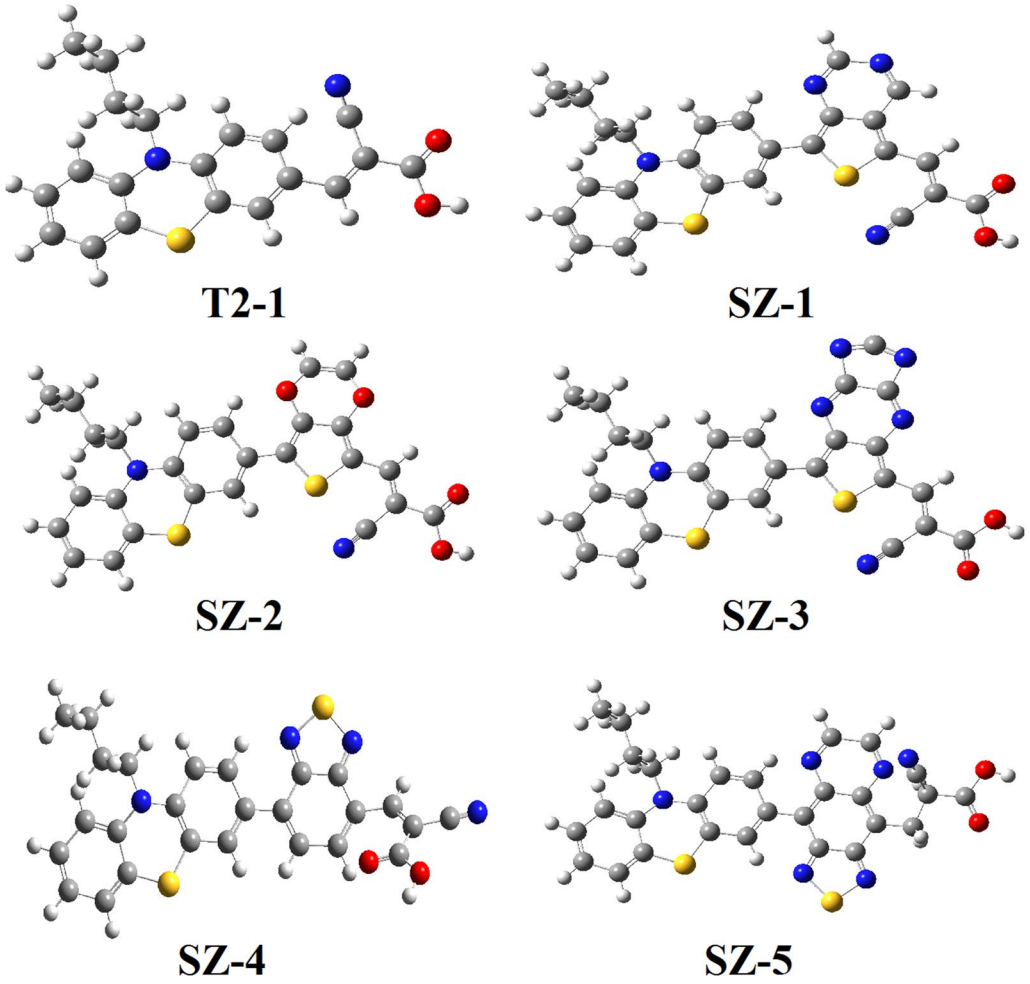

Fig. 1 Optimized ground state geometries of the dye molecules in solvent phase obtained at the B3LYP/6-31G(d) level of theory.

Table I Some specific dihedral angles of the optimized dyes

Dye molecules	Dihedral angle (°)	
	C1-C2-C3-C4	C1-C2-C3-C4
T2-1	− 179.9965	180.0002
SZ-1	− 179.9894	179.9985
SZ-2	− 179.9236	179.9854
SZ-3	− 179.9469	179.9913
SZ-4	− 179.8793	179.9729
SZ-5	− 179.9989	179.9565

intensities since the S1-S0 electronic transitions were found to have high λ_{emi} and excitation energy. The strong absorption band in SZ-3 is attributed to the π-π* electronic transition because it was discovered that SZ-3 has a greater λ_{emi} at 950 nm, which is 419 nm higher than the T2-1 absorption λ_{max}. Table IV demonstrates that good electron injection and CT properties of the DSSCs are anticipated for all PTZ dye compounds.

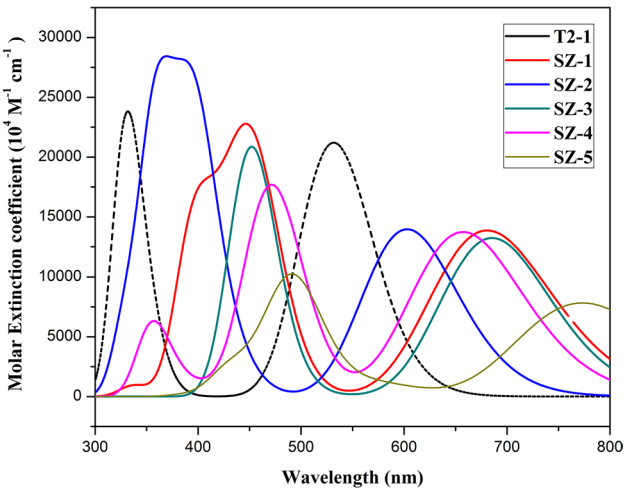

Fig. 2 UV–vis absorption spectra of organic dyes in THF solution.

Intramolecular Charge Transfer Analysis

The electronic structure and molecular distribution pattern of the SZ-1–SZ-5 dyes have been further studied using the frontier MO (FMO) theory. The HOMO and LUMO of MO theory are of particular relevance in this regard since they may be advantageous in the potential CT processes. The charge distribution in the MOs is dispersed on the HOMO and LUMO levels during the photoexcitation process, and it is also partially distributed to the π-spacers. The electronic density maps of the HOMOs and LUMOs are shown in 3D-optimized structures in Fig. 4. The image clearly shows that the HOMO to LUMO electron transition can predict the emergence of desirable charge-separated states for the specified dyes and that the HOMO-LUMO energy levels are related to CT processes from D to A. According to the MO theory, the overlap between the HOMO and LUMO transition determines the distribution of electron density in the σ1s MO, and the D-A moiety exhibits the strongest induction effects and π-spacer groups. As a result, we conclude that the conduction band edge (CBE) of TiO_2 material exhibits substantial interactions between the electron-D and A.

Because it is considered to be more suitable for solar cell applications, the LUMO energy level was compared with the potential CBE of TiO_2. These measurements reveal a shorter electron transport time and longer lifetime of photoexcited charge carriers. We have taken into consideration a CBE of TiO_2 at the calculation values that are comparable to the experimental data (−4.0 eV). The electrolyte redox potential (I/I_3^-) and the HOMO level capacity to penetrate the mesoporous semiconductor layer are both highly effective and have good long-term stability. Low dye regeneration contribute to faster photoelectrons injection into the CB. All the SZ-1–SZ-5 dyes meet the molecular excited energy states necessary for their ability to function as photosensitizers. The LUMO level is specifically situated above the oxide CBE of the TiO_2 surface, enabling the CT process from the dye sensitizers to the semiconductor and electrolyte. Furthermore, the efficient regeneration of oxidized states is made possible by the fact that the HOMO level is lower than the (−4.8 eV) redox shuttle. Because all of the proposed molecules have identical relative transition energy levels, it is impossible to predict which one will effectively offer a CT to the oxidation state. With a LUMO of −4.93 eV, the SZ-3 dye is closest to the TiO_2 conduction band, as seen in Fig. 5.

Table II Computed electronic transitions, absorption maxima (λ_{max} in nm), oscillator strengths (*f* in a.u.), electronic excitation energies (*E* in eV) and orbital contributions (%) of SZ-1–SZ-5 dyes using TD-DFT at B3LYP/6-31G(d,p) level

Dyes	Electronic transition	λ_{max}(nm)	*f* (a.u.)	*E* (eV)	Orbital contribution (%)
T2-1	$S_0 \rightarrow S_1$	531	0.292	2.33	H->L (99%)
SZ-1	$S_0 \rightarrow S_1$	680	0.181	1.82	H->L (100%)
SZ-2	$S_0 \rightarrow S_1$	602	0.172	2.05	H->L (100%)
SZ-3	$S_0 \rightarrow S_1$	810	0.197	1.53	H->L (100%)
SZ-4	$S_0 \rightarrow S_1$	657	0.182	1.88	H->L (99%)
SZ-5	$S_0 \rightarrow S_1$	648	0.108	1.91	H->L (100%)

H HOMO, *L* LUMO

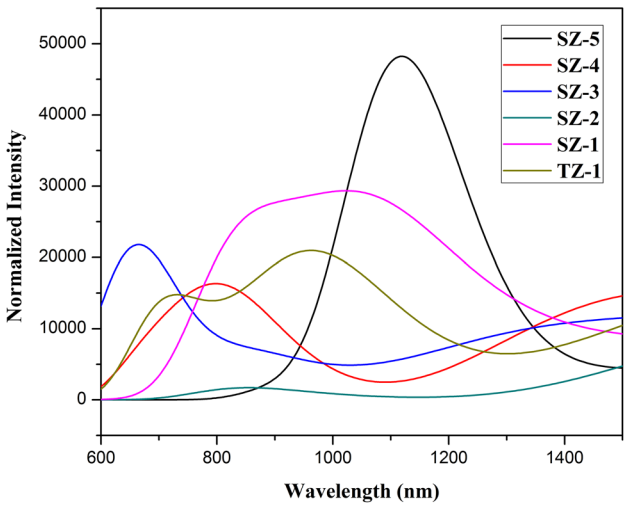

Fig. 3 Emission spectra of the all dyes in THF solution.

Table III Calculated oxidation and reduction potential energies (E^{dye}, E^{dye^*} in eV), vertical transition energy (*E* in eV), free energy of electron injection (in eV), regeneration (in eV), open-circuit photovoltage (eV_{OC} in eV), light-harvesting efficiency (*LHE* in a.u.), first-order hyperpolarizability (β in e.s.u.) and dipole moment (μ_{normal} in debye) of SZ-1–SZ-5 dyes

Dyes (in eV)	*E* (in eV)	E^{dye} (in eV)	E^{dye^*} (in eV)	ΔG_{reg} (in eV)	eV_{OC} (in eV)	ΔG_{inject} (in eV)	*LHE* (a.u.)	β (e.s.u.)	μ_{normal}(in Debye)
T2-1	2.74	5.05	2.72	0.25	1.69	1.28	0.49	1.941	4.2320
SZ-1	2.16	5.32	3.49	0.52	0.84	1.51	0.35	1.342	3.7547
SZ-2	2.38	5.17	3.11	0.37	1.21	1.89	0.33	2.043	7.7876
SZ-3	1.27	5.20	3.67	0.40	0.93	1.34	0.37	2.765	7.8431
SZ-4	2.25	5.29	3.40	0.49	0.96	1.60	0.35	1.613	7.0772
SZ-5	1.68	5.06	3.14	0.26	0.62	1.25	0.23	2.395	6.2543

Table IV Computed electronic transitions, emission spectra (λ_{emi} in nm), oscillator strengths (f in a.u.), electronic excitation energies (E in eV) and orbital contributions (%) of all designed molecules using TD-DFT at B3LYP/6-31G(d,p) level

Dyes	Electronic transition	λ_{emi}(nm)	f (a.u.)	E (eV)	Orbital contribution (%)
T2-1	$S_1 \rightarrow S_0$	619	0.664	2.00	H- > L (99%)
SZ-1	$S_1 \rightarrow S_0$	944	0.114	1.31	H-2- > L (95%)
SZ-2	$S_1 \rightarrow S_0$	915	0.004	1.35	H- > L + 1 (52%), H-2- > L (43%)
SZ-3	$S_1 \rightarrow S_0$	950	0.005	1.30	H-4- > L (18%), H-2- > L (79%)
SZ-4	$S_1 \rightarrow S_0$	869	0.080	1.42	H- > L (99%)
SZ-5	$S_1 \rightarrow S_0$	811	0.092	1.52	H- > L (45%), H-3- > L (51%)

H HOMO, *L* LUMO

Density of States

Using density of states (DOS) calculations of the SZ-1–SZ-5 molecules along with their estimation onto the component parts of developed dyes and compared with T2-1 dye, we are able to obtain a clearer understanding of the electron injection mechanism. The T2-1, or the point at which the energy band gaps of HOMOs and LUMOs are zero, is represented by the black line. Consequently, clarification of the differences in energy conversion due to macrocycle cavity replacement and elongating the bond distances of the π-conjugation system of the D-π-A dyes is required in the current density spectrum. The DOS of a molecular system denotes the region of power-level states per interspaces that are attainable states that electrons can occupy. Since there are multiple energy levels available for electron occupation in the high-energy area of the DOS at a given energy stage, superlinear scaling with the extremely efficient conversion is possible. The computed DOS spectrum of the dye molecules is intended to demonstrate the influence of the metal alternative as well as the greatest effect of lengthening the strong π-conjugation. As seen in Fig. 6, the DOS becomes more abundant close to Fermi degrees when moving from SZ-1 to SZ-5 molecules, where additional profound vales arise on the two sides close to the Fermi levels. This illustrates the main impact of increasing the strong bond distance of the π-spacer system on enhancing the performance of solar cells.

Nonlinear Optical Properties

The quality of intermolecular interactions, total cross sections of different scattering and frequency-mixing methods, as well as the NLO properties of the molecular system, can all be used to determine the first static hyperpolarizabilities.[41,42] According to reports, a novel hemicyanine sensitizer framework with outstanding photoelectric conversion typically possesses great optical properties. Calculations were made for the electro-optics and hyperpolarizabilities of SZ-1–SZ-5 compounds in order to examine the links between molecular structures. Hyperpolarizabilities can be calculated using TD-DFT-dependent sum-over states (SOS), coupled-perturbed Hartree–Fock (CPHF) and finite perturbation (FP) theory. However, very large basis sets for dyes cannot afford to use CPHF, FP, and SOS procedures since they are too expensive. Here, using B3LYP at the 6-31G(d,p) level of theory, we numerically differentiate to derive the static first-order hyperpolarizability, which can be calculated by Eq. 1.[43]

$$\beta = \left[\left(\beta_{xxx}, \beta_{xyy}, \beta_{xzz}\right)^2 + \left(\beta_{xxy}, \beta_{xzz}, \beta_{yzz},\right)^2 + \left(\beta_{xxz}, \beta_{zyy}, \beta_{zzz}\right)^2\right]^{1/2} \quad (1)$$

where $\beta_{xxx}, \beta_{xyy}, \beta_{xzz}, \beta_{xxy}, \beta_{xzz}, \beta_{yzz}, \beta_{xxz}, \beta_{zyy}, \beta_{zzz}$ are the tensor components of first hyperpolarizability of designed dyes, respectively. Hyperpolarizability is inversely proportional to E. Table III shows that the hyperpolarizability value of an SZ-3 molecule is 2.765×10^{-28} e.s.u. (E is 1.27 eV obtained from TD-DFT method).

Photovoltaic Properties

In general, photosensitizers determine the PCE of DSSCs. The spacer effects of the D-π-A structure are the primary structural component of the most effective metal-free dyes. Different π-bridge groups inside the D-π-A structure can change the photophysical characteristics of planned dyes. As a result, TD-DFT computation is employed in this study, which is an effective way of identifying the optimum electronic structural features of SZ-1–SZ-5 dyes in comparison to other sophisticated quantum chemical techniques. The orbitals have been shown to be ideal for the features of computational survey and interpretations.

We are aware that the intensity of incident light (P_{INC}), open-circuit voltage (V_{OC}), fill factor (FF) and short-circuit current density (J_{SC}) all affect the PCE of solar cell characteristics, and they can be calculated by Eq. 2.[44]

$$\eta = \frac{V_{OC} J_{SC} FF}{P_{INC}} \quad (2)$$

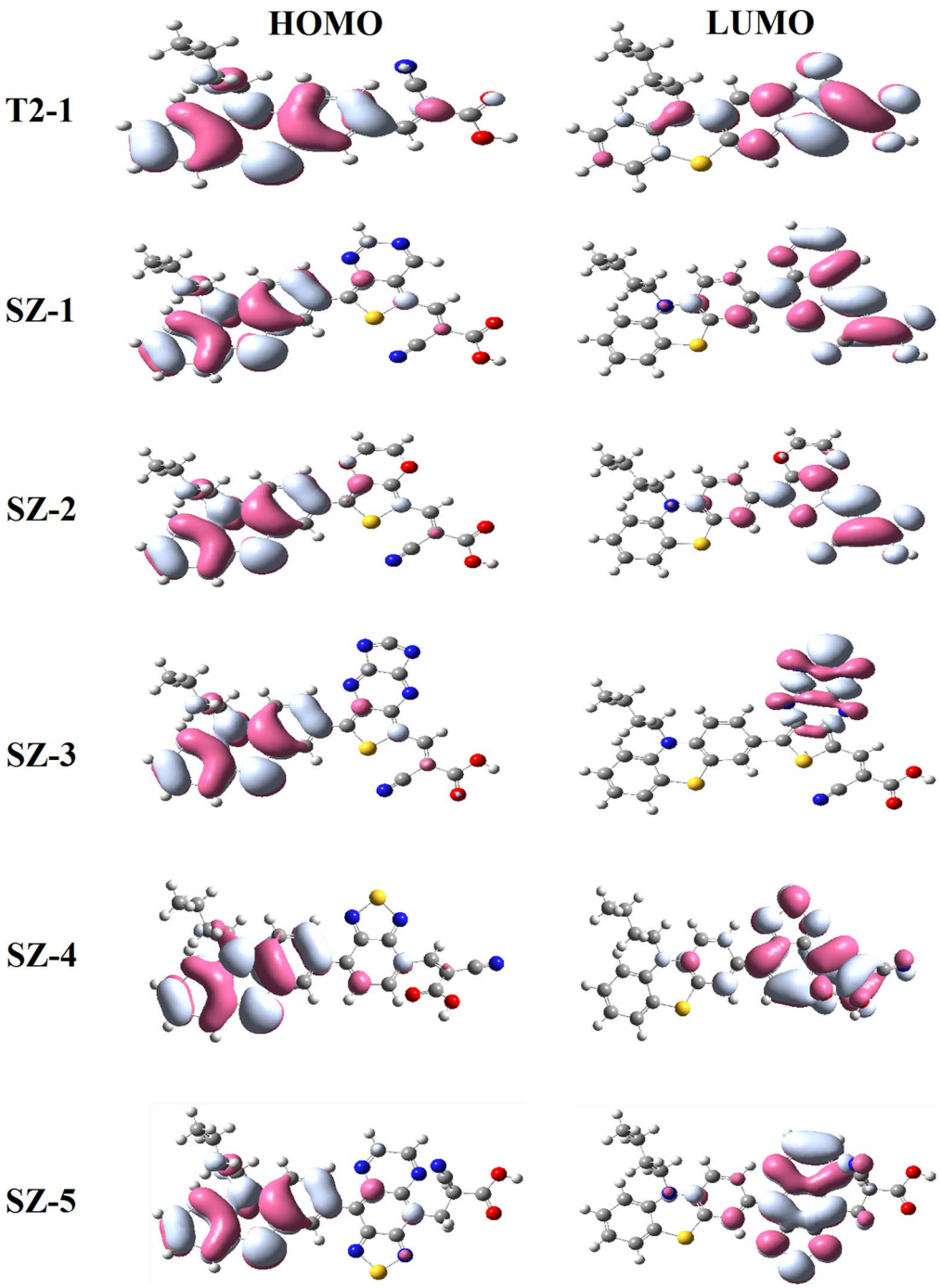

Fig. 4 Electron distributions of the HOMOs and LUMOs.

The following Eq. 3 can be used to estimate V_{OC} in DSSCs,

$$V_{OC} = \frac{E_{CB}}{q} + \frac{kT}{q} \ln\left(\frac{n_C}{N_{CB}}\right) - \frac{E_{redox}}{q} \tag{3}$$

where the V_{OC} of a DSSC is determined by the energy LUMO difference between the quasi-Fermi level of p-type

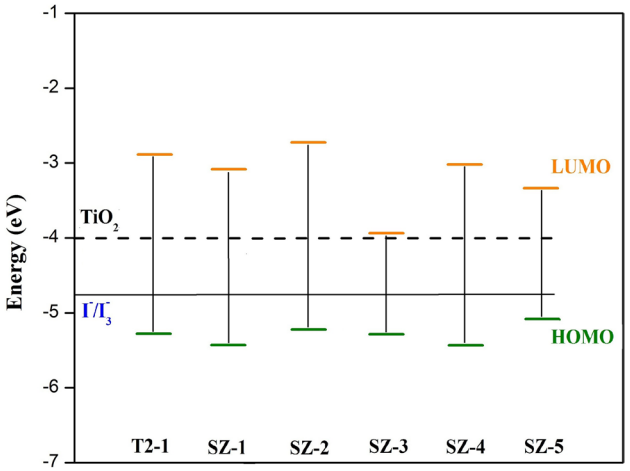

Fig. 5 FMO energy level diagram of the SZ(1–5) dyes.

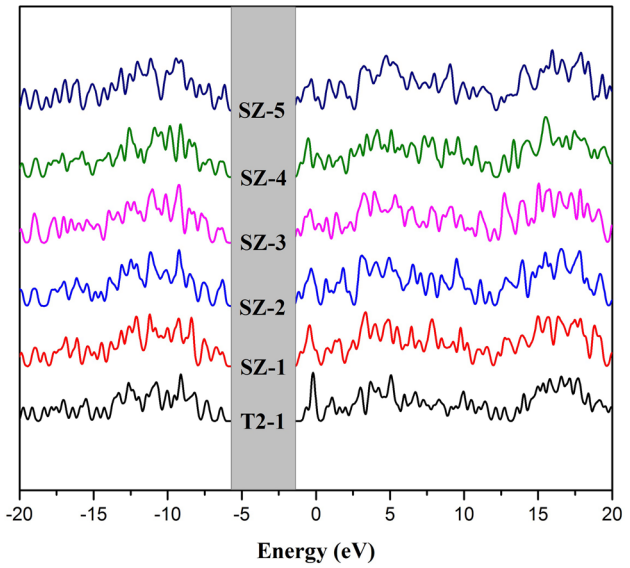

Fig. 6 DOS spectrum of the SZ(1–5) dyes.

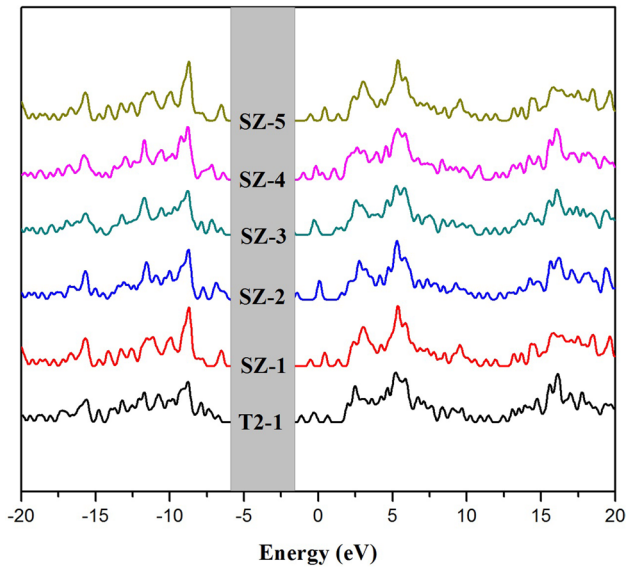

Fig. 7 DOS of all dye@TiO_2 complexes.

semiconductor substrate CBE of TiO_2 and the redox potential of the electrolyte. It is assumed that the I^-/I_3^- solution will be utilized as the redox electrolyte in DSSCs. ΔCB is the main influencing factor of V_{OC}, which is calculated using the following Eq. 4,

$$\Delta CB = -\frac{q\mu_{normal}\gamma}{\varepsilon_0\varepsilon} \tag{4}$$

where q is the elementary charge, γ is the molecular outermost level concentration, μ_{normal} denotes the total dipole moment (μ_{normal}) of different π-conjugated dye molecules perpendicular to the surface of the TiO_2 and ε_0, ε is the dielectric constant. It is obvious that a high μ_{normal} will cause the CBE to shift more, which results in a higher value for V_{OC}. Compared to T2-1, the SZ-3 dye molecule (7.8431 D) has the highest μ_{normal} of an excellent electronic transition, as indicated in Table IV, which may contribute to the high PCE of DSSCs. The formula from the literature was used to compute the maximum theoretical eV_{OC} of the dyes, and the corresponding values are provided in Table III.[45] From the table, SZ-1–SZ-5 dye values are 0.84, 1.21, 0.93, 0.96 and 0.62 eV, respectively. Table III shows that the absolute eV_{OC} values of SZ-1–SZ-5 indicate a promising and capable electron injection mechanism. Taking into account values of eV_{OC} , all the dyes may have higher V_{OC} of the organic solar cell. These findings show that all sensitizers may make excellent candidates for DSSCs.

The following Eq. 5 can be used to express J_{SC} parameters, which is another method of increasing PCE.[46]

$$J_{SC} = \int_{\lambda} LHE(\lambda)\Phi_{inject}\eta_{collect}d\lambda \tag{5}$$

where *LHE(λ)* is a measure of light harvesting efficiency related to UV–Vis wavelength, Φ_{inject} is the electron injection efficiency from the excited state dye and $\eta_{collect}$ refers to the charge collection efficiency. Since the designed organic sensitizers are the only difference between DSSC electrodes, $\eta_{collect}$ can be assumed to remain constant.[47] The *f* of the absorption spectra allows for the calculation of *LHE(λ)*.[48] Table III indicates that the *LHE* of SZ-3 dye molecules (0.37 a.u.) has a high value when compared to other dyes. The driving force for the fast electron injection (ΔG_{inject}) from excited dyes to the CBE of TiO_2 was directly related to these values. According to the literature, to achieve good

performance, ΔG_{inject} must be more than 0.2 eV.[49] This can be summarized by the following Eq. 6.[50]

$$\Delta G_{inject} = E^{dye^*} - E^{TiO_2} \quad (6)$$

where E^{dye^*} represents the reduction potential of the dyes, E_{CB} is the energy value of CBE (−4.0 eV) and the electronic state energies. Table IV lists the calculated ΔG_{inject} values for all the dyes examined. We can see that these excited state dyes have an adequate driving power for rapid charge injection because the corresponding values of ΔG_{inject} for SZ-1–SZ-5 are significantly better than 0.2 eV. However, a high value may come before energy redundancy, which can be provided by a smaller ΔG_{inject} and larger thermalization losses.[51,52] The dye regeneration efficiency (ΔG_{reg}), which can be determined using Eq. 7, also affects J_{SC} of DSSCs.[53]

$$\Delta G_{reg} = E_{redox} - E^{dye} \quad (7)$$

where E^{dye} is the oxidation potential of the dyes and E_{redox} is the redox potential of the dyes (at −4.8 eV). According to the review by Robson, the charge/electron movement in the

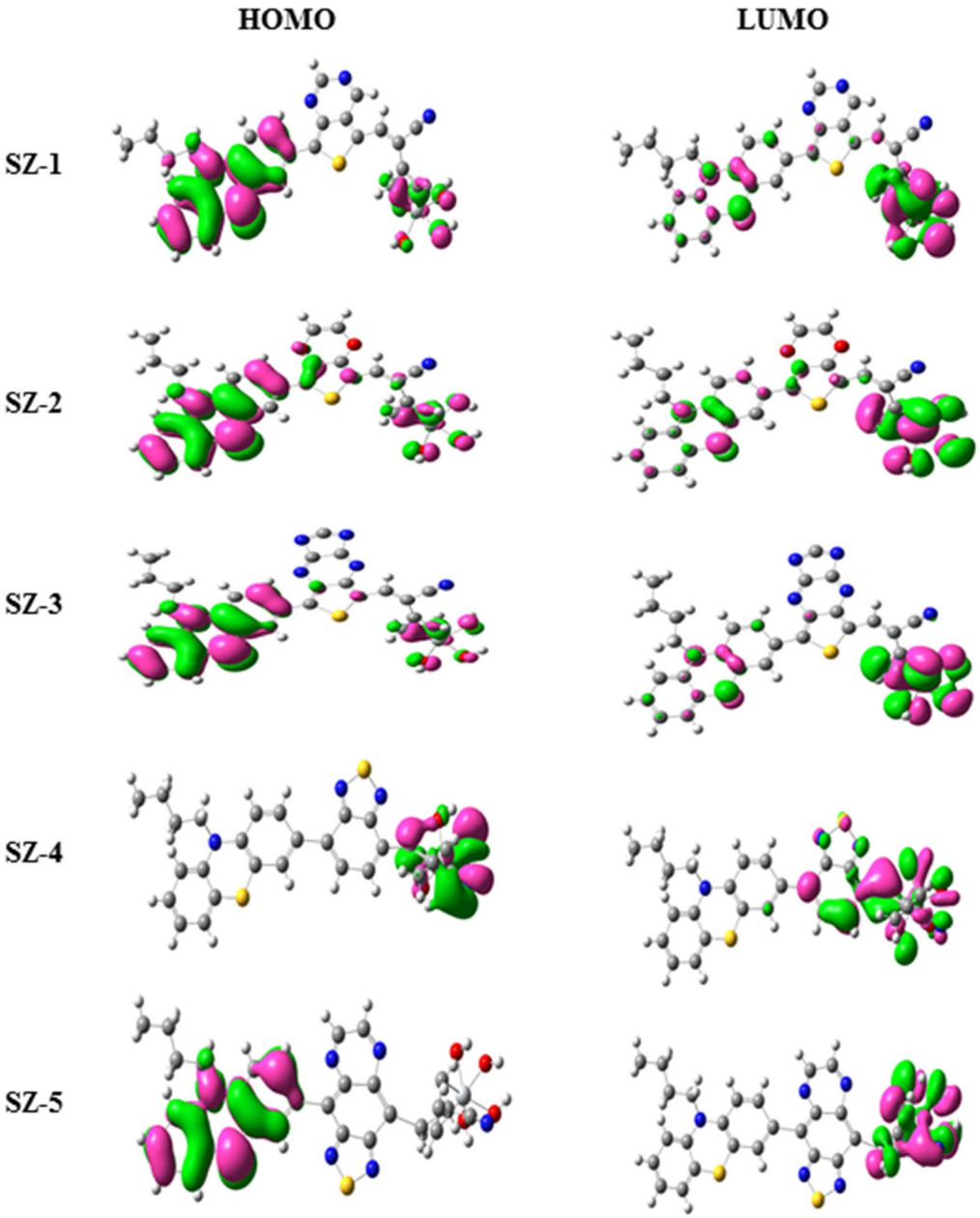

Fig. 8 Representation of the all dye@TiO_2 complexes of HOMOs and LUMOs were obtained at the TDB3LYP/6-31G(d) level.

Table V Simulated oxidation and reduction potential energies (E^{dye}, E^{dye^*} in eV), vertical transition energy (E in eV), free energy of electron injection (in eV), regeneration (in eV), open-circuit photovoltage (eV_{OC} in eV), oscillator strength (f in a.u.) and light-harvesting efficiency (*LHE* in a.u.) of the SZ-1–SZ-5 with Ti dyes

Dyes (eV)	E (eV)	E^{dye} (eV)	E^{dye^*} (eV)	ΔG_{reg} (eV)	eV_{OC} (eV)	ΔG_{inject} (eV)	f (a.u.)	LHE (a.u.)
T2-1	0.4535	5.10	5.79	5.34	0.99	1.43	0.006	0.014
SZ-1	0.6043	5.47	4.86	0.67	1.47	0.67	0.002	0.004
SZ-2	0.5448	5.67	5.12	0.87	1.67	0.55	0.073	0.155
SZ-3	0.8362	5.71	4.87	0.91	1.71	0.65	0.007	0.016
SZ-4	1.3631	4.76	3.39	0.04	0.76	1.40	0.009	0.021
SZ-5	1.0310	5.03	3.99	0.23	1.03	1.45	0.003	0.007

TiO_2 surface and the ΔG_{reg} of the oxidized dyes can greatly increase the high conversion efficiency of the DSSCs.[54] The augmentation of regeneration, which is found to facilitate the increase of J_{SC}, occurs because of the stronger electron driving forces for electron injection of the SZ-3 dye and regeneration of the oxidized dye. The best candidate among all the SZ-1–SZ-5 dyes is the SZ-3 molecule, which has the best performance on PV parameters such as $\lambda_{\max}$, *LHE*, J_{SC}, μ_{normal}, eV_{OC} and achieves tolerable stability between conflicting factors. In light of this, the SZ-3 molecule will be a strong candidate for excellent performance in DSSCs.

Impact of the Semiconductor

We next compute the DOS spectrum of the dyes tied to Ti complexes together with their prediction onto the various components of the SZ-1–SZ-5 molecules to gain a better understanding of the electron injection mechanism. The centre of the Ti semiconductor HOMO-LUMO energy levels, which is put at 0 eV in Fig. 7, is known as the quasi-Fermi level of a solid state. The HOMOs and LUMOs were studied and are shown in Fig. 8 to help understand the type of electron density. This graph shows that the PTZ group is primarily stabilized by the HOMOs, while the semiconductor is primarily stabilized by the LUMOs.

We use this work as a chance to theoretically calculate the dyes associated with the Ti complex. In order to ensure that all of the dyes are neutral groups, we assume that the dyes are restricted to a bridge Ti atom and the SZ-1–SZ-5 groups. Using the DFT ground state approach, Peng and colleagues discovered a similar impact in this model.[55] The following are the results of the full theoretical approach. We analyse the impact of the Ti semiconductor collision on the ΔG_{inject} parameter and compute the semiconductor effects on the important parameters. The charge injection forces and electron transfer are connected to the $\lambda_{\max}$,E_{ox}^{dye} E^{dye} and E^{dye^*} E_{ox}^{dye*} needed to evaluate the free energy change. We have estimated all of the PV parameters shown in Table V using both the Ti model and the calculated variation of the ΔG_{inject},E_{ox}^{dye}, E^{dye} and E^{dye^*} (in eV). The positions of the LUMO energy level and the CB of Ti-based materials are particularly crucial for the highest solar energy transfer process of PV devices because the higher energy levels of the electrons are influenced by injection rates. Unfortunately, it is exceedingly difficult to obtain accurate estimates of these energies, the absolute values, and the position of the LUMOs above or below the CB edge compared to the Ti-CB state at the current levels of theory.

Conclusions

In conclusion, theoretical research was conducted to investigate the use of DFT and TD-DFT calculations to estimate the structural, electronic and photophysical properties of PTZ-based SZ-1–SZ-5 molecules for DSSCs. When compared to T2-1 dye, the metal-free SZ-1–SZ-5 dyes performed well in terms of their J_{SC}, eV_{OC} properties. Our findings showed that the HOMO-LUMO gap in these dyes was lower than that in molecules reported in the literature. Specifically, SZ-3 dye exhibits a reduction in the HOMO-LUMO energy gap, an increase in optical activity and noticeably enhanced PV characteristics. The improvement of DSSCs based on PTZ dye was therefore thought to have been greatly influenced by the results of this investigation. Finally, PTZ derivatives demonstrate how π-spacer groups can be appropriately adjusted for use with organic PV in DSSC applications by changing their D-π-A structure.

Acknowledgments The authors extend their appreciation to the Research Centre for Advanced Materials Science (RCAMS), King Khalid University, Saudi Arabia, for funding this work under Grant Number RCAMS/KKU/040-22.

Conflict of interest The authors declared that there is no conflict of interest.

References

1. J.H. Kim, D.H. Kim, J.H. So, and H.J. Koo, Toward eco-friendly dye-sensitized solar cells (DSSCs): Natural dyes and aqueous electrolytes. *Energies* 15, 219 (2022).
2. J. Zou, Y. Wang, G. Baryshnikov, J. Luo, X. Wang, H. Ågren, and C. Li, Xie, Y, Efficient dye-sensitized solar cells based on a new class of doubly concerted companion dyes. *ACS Appl. Mater. Interfaces* 14, 33274 (2022).
3. S.C. Pradhan, J. Velore, A. Hagfeldt, and S. Soman, Probing photovoltaic performance in copper electrolyte dye-sensitized solar cells of variable TiO_2 particle size using comprehensive interfacial analysis. *J. Mater. Chem. C* 10, 3929 (2022).
4. B. Oregan and M. Grätzel, *Nature* 353, 737 (1991).
5. A. Yella, H.W. Lee, H.N. Tsao, C. Yi, A.K. Chandiran, M.K. Nazeeruddin, E.W.G. Diau, C.Y. Yeh, S.M. Zakeeruddin, and M. Grätzel, Porphyrin-sensitized solar cells with cobalt (II/III)-based redox electrolyte exceed 12 percent efficiency. *Sci.* 334, 629 (2011).
6. P.M. Anbarasan, A. Arunkumar, and M. Shkir, Computational investigations on efficient metal-free organic D-π-A dyes with different spacers for powerful DSSCs applications. *Mol. Simul.* 48, 140 (2022).
7. A. Arunkumar and P.M. Anbarasan, Optoelectronic properties of a simple metal-free organic sensitizer with different spacer groups: quantum chemical assessments. *J. Electron. Mater.* 48, 1522 (2019).
8. N. Naeem, R.A. Shehzad, M. Ans, M.S. Akhter, and J. Iqbal, Dopant free triphenylamine-based hole transport materials with excellent photovoltaic properties for high-performance perovskite solar cells. *Energy Technol.* 10, 2100838 (2022).
9. S.G. Kim, S.H. Lee, I.S. Yang, Y.J. Park, K. Park, J.W. Lee, and N.G. Park, Effect of fluorine substitution in a hole dopant on the photovoltaic performance of perovskite solar cells. *ACS Energy Lett.* 7, 741 (2022).
10. H. Liu, P. Cheng, Q. Chen, and X. Liu, Modulation of planarity on carbazole derivatives-based hole transport materials for perovskite solar cells: a theoretical and experimental research. *J. Electron. Mater.* 51, 1778 (2022).
11. R. Govindarasu, M.K. Subramanian, A. Arunkumar, P.M. Anbarasan, and M. Shkir, D-π-A manufactured organic dye molecules with different spacers for highly efficient reliable DSSCs via computational analysis. *Mol. Simul.* 48, 584 (2022).
12. K.K. Chenab, M.R.Z. Meymian, and S.M. Qashqay, Charge recombination suppression in dye-sensitized solar cells by tuning the dielectric constant of triphenylamine dyes with altering π-bridges from naphthalene to anthracene units. *Phys. Chem. Chem. Phys.* 24, 19595 (2022).
13. H. Katsuyama, R. Sumita, R. Yamakado, and S. Okada, Reactions introducing 4-cyano-5-dicyanomethylene-2-oxo-3-pyrrolin-3-yl group to 4-ethynyl-N, N-dialkylaniline derivatives and characterization of the resulting dyes. *Dyes Pigm.* 199, 110103 (2022).
14. S.M. Wagalgave, M. Al-Kobaisi, S.V. Bhosale, and S.V. Bhosale, Donor-acceptor-donor π-conjugated material derived from merocyanine-diketopyrrolopyrrole: design, synthesis and photovoltaic applications. *J. Electroanal. Chem.* 915, 116341 (2022).
15. M.S. Ebied, M. Dongol, M. Ibrahim, M. Nassary, S. Elnobi, and A.A. Abuelwafa, Structural and optical properties of nanocrystalline 3-(2-benzothiazolyl)-7-(diethylamino) coumarin (C6) thin films for optoelectronic application. *J. Electron. Mater.* 51, 5770 (2022).
16. R. Pradhan, A. Agrawal, B.P. Bag, R. Singhal, G.D. Sharma, and A. Mishra, High-efficiency ternary organic solar cells enabled by synergizing dicyanomethylene-functionalized coumarin donors and fullerene-free acceptors. *ACS Appl. Energy Mater.* 5, 9020 (2022).
17. M.L. Han, Y.Z. Zhu, S. Liu, Q.L. Liu, D. Ye, B. Wang, and J.Y. Zheng, The improved photovoltaic performance of phenothiazine-dithienopyrrole based dyes with auxiliary acceptors. *J. Power Sources* 387, 117 (2018).
18. Z.S. Huang, C. Cai, X.F. Zang, Z. Iqbal, H. Zeng, D.B. Kuang, L. Wang, H. Meier, and D. Cao, Effect of the linkage location in double branched organic dyes on the photovoltaic performance of DSSCs. *J. Mater. Chem. A* 3, 1333 (2015).
19. A. Arunkumar, M. Deepana, S. Shanavas, R. Acevedo, and P.M. Anbarasan, Computational investigation on series of metal-free sensitizers in tetrahydroquinoline with different π-spacer Groups for DSSCs. *ChemistrySelect* 4, 4097 (2019).
20. M.Y. Mehboob, R. Hussain, M.U. Khan, M. Adnan, M.A. Ehsan, A. Rehman, and M.R.S.A. Janjua, Quantum chemical design of near-infrared sensitive fused ring electron acceptors containing selenophene as π-bridge for high-performance organic solar cells. *J. Phys. Org. Chem.* 34, 4204 (2021).
21. M. Rafiq, M. Salim, S. Noreen, R.A. Khera, S. Noor, U. Yaqoob, and J. Iqbal, End-capped modification of dithienosilole based small donor molecules for high performance organic solar cells using DFT approach. *J. Mol. Liq.* 345, 118138 (2022).
22. M.U. Khan, R. Hussain, M.Y. Mehboob, M. Khalid, M.A. Ehsan, A. Rehman, and M.R.S.A. Janjua, First theoretical framework of Z-shaped acceptor materials with fused-chrysene core for high performance organic solar cells. *Spectrochim. Acta A Mol. Biomol. Spectrosc.* 245, 118938 (2021).
23. D.D.Y. Setsoafia, K.S. Ram, H. Mehdizadeh-Rad, D. Ompong, V. Murthy, and J. Singh, DFT and TD-DFT calculations of orbital energies and photovoltaic properties of small molecule donor and acceptor materials used in organic solar cells. *J. Renew. Mater.* 10, 2553 (2022).
24. M. Rani, J. Iqbal, R.F. Mehmood, E.U. Rashid, S. Rani, M. Raheel, and R.A. Khera, Strategies toward the end-group modifications of indacenodithiophene based non-fullerene small molecule acceptor to improve the efficiency of Organic solar Cells; a DFT study. *Comput. Theor. Chem.* 113747 (2022).
25. M.R. Janjua, Theoretical understanding and role of guest π-bridges in triphenylamine-based donor materials for high-performance solar cells. *Energ. Fuel.* 35, 12451 (2021).
26. A. Arunkumar, S. Shanavas, and P.M. Anbarasan, First-principles study of efficient phenothiazine-based D-π-A organic sensitizers with various spacers for DSSCs. *J. Comput. Electron.* 17, 1410 (2018).
27. D. Nebbach, F. Agda, S. Kaya, F. Siddique, T. Lakhlifi, M.A. Ajana, and M. Bouachrine, Non-fullerene acceptor IDIC based on indacinodithiophene used as an electron donor for organic solar cells: a computational study. *J. Mol. Liq.* 348, 118289 (2022).
28. A. Arunkumar, M. Prakasam, and P.M. Anbarasan, Influence of donor substitution at D-π-A architecture in efficient sensitizers for dye-sensitized solar cells: first-principle study. *Bull. Mater. Sci.* 40, 1389 (2017).
29. M. Rani, J. Iqbal, R.F. Mehmood, S.J. Akram, K. Ghaffar, Z.M. El-Bahy, and R.A. Khera, Engineering of A-π-D-π-A system based non-fullerene acceptors to enhance the photovoltaic properties of organic solar cells; A DFT Approach. *Chem. Phys. Lett.* 139750 (2022).
30. P.M. Anbarasan, A. Arunkumar, and M. Shkir, Computational analysis of carbazole-based newly efficient D-π-A organic spacer dye derivatives for dye-sensitized solar cells. *Struct. Chem.* 33, 1097 (2022).
31. A. Arunkumar, S. Shanavas, R. Acevedo, and P.M. Anbarasan, Computational analysis on D-π-A based perylene organic efficient sensitizer in dye-sensitized solar cells. *Opt. Quant. Electron.* 52, 1 (2020).

32. A. Arunkumar, S. Shanavas, R. Acevedo, and P.M. Anbarasan, Quantum chemical investigation of modified coumarin-based organic efficient sensitizers for optoelectronic applications. *Eur. Phys. J. D* 74, 1 (2020).
33. H. Tian, X. Yang, R. Chen, Y. Pan, L. Li, A. Hagfeldt, and L. Sun, Phenothiazine derivatives for efficient organic dye-sensitized solar cells. *Chem. Commun.* 36, 3741 (2007).
34. X. Zhang, F. Gou, J. Shi, H. Gao, C. Xu, Z. Zhu, and H. Jing, Molecular engineering of new phenothiazine-based D-A-π-A dyes for dye-sensitized solar cells. *RSC Adv.* 6, 106380 (2016).
35. M. Sharma, N. Sharma, P.A. Alvi, S.K. Gupta, and C.M.S. Negi, P3HT-rGO composites for high-performance optoelectronic devices. *Opt. Mater.* 127, 112326 (2022).
36. M. Sharma, P.A. Alvi, S.K. Gupta, and C.M.S. Negi, The optoelectronic behavior of reduce graphene oxide-carbon nanotube nanocomposites. *Synth. Met.* 281, 116892 (2021).
37. K. Sharma, V. Sharma, and S.S. Sharma, Dye-sensitized solar cells: fundamentals and current status. *Nanoscale Res. Lett.* 13, 1 (2018).
38. M.J. Frisch, G.W. Trucks, H.B. Schlegel, G.E. Scuseria, M.A. Robb, J.R. Cheeseman, G. Scalmani, V. Barone, B. Mennucci, G.A. Petersson, H. Nakatsuji, M. Caricato, X. Li, H.P. Hratchian, A.F. Izmaylov, J. Bloino, G. Zheng, J.L. Sonnenberg, M. Hada, M. Ehara, K. Toyota, R. Fukuda, J. Hasegawa, M. Ishida, T. Nakajima, Y. Honda, O. Kitao, H. Nakai, T. Vreven, J.A. Montgomery Jr., J.E. Peralta, F. Ogliaro, M.J. Bearpark, J. Heyd, E.N. Brothers, K.N. Kudin, V.N. Staroverov, R. Kobayashi, J. Normand, K. Raghavachari, A.P. Rendell, J.C. Burant, S.S. Iyengar, J. Tomasi, M. Cossi, N. Rega, N.J. Millam, M. Klene, J.E. Knox, J.B. Cross, V. Bakken, C. Adamo, J. Jaramillo, R. Gomperts, R.E. Stratmann, O. Yazyev, A.J. Austin, R. Cammi, C. Pomelli, J.W. Ochterski, R.L. Martin, K. Morokuma, V.G. Zakrzewski, G.A. Voth, P. Salvador, J.J. Dannenberg, S. Dapprich, A.D. Daniels, O. Farkas, J.B. Foresman, J.V. Ortiz, J. Cioslowski, and D.J. Fox, *Gaussian 09* (Wallingford: Gaussian Inc., 2009).
39. A.D. Becke, *J. Chem. Phys.* 98, 5648 (1993).
40. C. Lee, W. Yang, and R.G. Parr, Development of the Colle-Salvetti correlation-energy formula into a functional of the electron density. *Phys. Rev. B* 37, 785 (1988).
41. M.A. Kern, D. Schubert, D. Sahi, M.M. Schöneweiß, I. Moll, A.M. Haugg, H.P. Dienes, K. Breuhahn, and P. Schirmacher, Proapoptotic and antiproliferative potential of selective cyclooxygenase-2 inhibitors in human liver tumor cells. *Hepatol.* 36, 885 (2002).
42. N. Bhala, J. Emberson, A. Merhi, S. Abramson, N. Arber, J.A. Baron, C. Bombardier, C. Cannon, M.E. Farkouh, G.A. FitzGerald, and P. Goss, Vascular and upper gastrointestinal effects of non-steroidal anti-inflammatory drugs: meta-analyses of individual participant data from randomised trials. *Lancet* 382, 769 (2013).
43. G. Maroulis and A.J. Thakkar, Polarizabilities and hyperpolarizabilities of carbon dioxide. *J. Chern. Phys.* 93, 4164 (1990).
44. T. Marinado, K. Nonomura, J. Nissfolk, M.K. Karlsson, D.P. Hagberg, L. Sun, S. Mori, and A. Hagfeldt, How the nature of triphenylamine-polyene dyes in dye-sensitized solar cells affects the open-circuit voltage and electron lifetimes. *Langmuir* 26, 2592 (2010).
45. S. Rühle, M. Greenshtein, S.G. Chen, A. Merson, H. Pizem, C.S. Sukenik, D. Cahen, and A. Zaban, Molecular adjustment of the electronic properties of nanoporous electrodes in dye-sensitized solar cells. *J. Phys. Chem. B* 109, 18907 (2005).
46. R. Tarsang, V. Promarak, T. Sudyoadsuk, S. Namuangruk, N. Kungwan, P. Khongpracha, and S. Jungsuttiwong, Triple bond-modified anthracene sensitizers for dye-sensitized solar cells: a computational study. *RSC Adv.* 5, 38130 (2015).
47. J. Zhang, H.B. Li, S.L. Sun, Y. Geng, Y. Wu, and Z.M. Su, Density functional theory characterization and design of high-performance diarylamine-fluorene dyes with different π spacers for dye-sensitized solar cells. *J. Mater. Chem.* 22, 568 (2012).
48. J. Preat, D. Jacquemin, C. Michaux, and E.A. Perpète, Improvement of the efficiency of thiophene-bridged compounds for dye-sensitized solar cells. *Chem. Phys.* 376, 56 (2010).
49. A. Islam, H. Sugihara, and H. Arakawa, Molecular design of ruthenium (II) polypyridyl photosensitizers for efficient nanocrystalline TiO_2 solar cells. *J. Photochem. Photobiol. A: Chem.* 158, 131 (2003).
50. R. Katoh, A. Furube, T. Yoshihara, K. Hara, G. Fujihashi, S. Takano, S. Murata, H. Arakawa, and M. Tachiya, Efficiencies of electron injection from excited N3 dye into nanocrystalline semiconductor (ZrO_2, TiO_2, ZnO, Nb_2O_5, SnO_2, In_2O_3) films. *J. Phys. Chem. B* 108, 4818 (2004).
51. Z. Ning, Q. Zhang, W. Wu, H. Pei, B. Liu, and H. Tian, Starburst triarylamine based dyes for efficient dye-sensitized solar cells. *J. Org. Chem.* 73, 3791 (2008).
52. T. Daeneke, A.J. Mozer, Y. Uemura, S. Makuta, M. Fekete, Y. Tachibana, N. Koumura, U. Bach, and L. Spiccia, Dye regeneration kinetics in dye-sensitized solar cells. *J. Am. Chem. Soc.* 134, 16925 (2012).
53. K.C.D. Robson, K. Hu, G.J. Meyer, and C.P. Berlinguette, Atomic level resolution of dye regeneration in the dye-sensitized solar cell. *J. Am. Chem. Soc.* 135, 1961 (2013).
54. Y. Liu, G. Yang, S. Sun, and Z. Su, Density functional theory investigation on the second-order nonlinear optical properties of chlorobenzyl-o-carborane derivatives. *Chin. J. Chem.* 30, 2349 (2012).
55. B. Peng, S. Yang, L. Li, F. Cheng, and J. Chen, A density functional theory and time-dependent density functional theory investigation on the anchor comparison of triarylamine-based dyes. *J. Chem. Phys.* 132, 034305 (2009).